

Communication

Power-over-Fiber with Simultaneous Transmission of Optical Carrier for a High Frequency Analog Signal over Standard Single-Mode Fiber

Andrei Varlamov, Peter Agruzov, Mikhail Parfenov, Aleksandr Tronev , Igor Ilichev, Anna Usikova and Aleksandr Shamrai * 

Department for Quantum Electronics, Ioffe Institute, St. Petersburg 194021, Russia

* Correspondence: achamrai@mail.ioffe.ru

Abstract: Efficient simultaneous transmission of light with a power of more than 2 W at a wavelength of 976 nm and an optical carrier for transmitting a high-frequency analog signal at a wavelength of 1550 nm over a distance of 1 km over a standard single-mode fiber was experimentally demonstrated. Electrical power up to 350 mW (5 V, 70 mA) was obtained from a multi-junction silicon photocell, resulting in the optical transmission efficiency of about 70% and a photocell efficiency of 25%. The power transmission did not affect the transmission of the high frequency analog signal. Key broadband analog transmission characteristics such as noise figure ($NF < 25$ dB) and spurious-free dynamic range ($SFDR_3 > 117$ dB/Hz^{2/3}) were achieved and were close to the fundamental shot noise limit. This approach is promising for powering a remote antenna unit in optical fronthaul architecture.

Keywords: power-over-fiber; fiber optic link; microwave photonics; antenna remoting; optical fronthaul architecture



Citation: Varlamov, A.; Agruzov, P.; Parfenov, M.; Tronev, A.; Ilichev, I.; Usikova, A.; Shamrai, A.

Power-over-Fiber with Simultaneous Transmission of Optical Carrier for a High Frequency Analog Signal over Standard Single-Mode Fiber.

Photonics **2023**, *10*, 17. <https://doi.org/10.3390/photonics10010017>

Received: 2 December 2022

Revised: 20 December 2022

Accepted: 21 December 2022

Published: 24 December 2022



Copyright: © 2022 by the authors. Licensee MDPI, Basel, Switzerland. This article is an open access article distributed under the terms and conditions of the Creative Commons Attribution (CC BY) license (<https://creativecommons.org/licenses/by/4.0/>).

1. Introduction

In the context of remote sound alert activation by optical means, the first proposals for the use of fiber-optic communication lines in power delivery simultaneously with information signal transmission date back to the late 1970s [1]. Since then, various systems based on the power-over-fiber (PoF) transmission procedure have been developed to supply those remote sensing and communication devices with power, which proved to be inconvenient in supplying them with electrical supplies [2–5].

The use of the PoF technique eliminates the need for batteries, solar panels, and long copper feeder wires at remote sites, which improves system reliability and security and reduces installation costs at remote sites. An optical fiber used in PoF is made of nonconductive material, and it is immune to electromagnetic interferences. Devices with PoF have a complete galvanic isolation to the ground potential and are immune to the ground potential rise effects.

The radio over fiber (RoF) technology, which transmits optically carried radio-frequency signals between the central station and a remote antenna unit (RAU), opens up new niches for the PoF application [6]. The benefits of the RoF technology are clear; remote devices are greatly simplified because the most expensive, heaviest, and power-consuming equipment is now centralized, and the centralization of wireless access points or radio base stations means that fewer radio resources are required to provide a given level of service. However, supplying power to multiple RAUs is becoming a challenge, especially in 5G wireless systems [7], where reducing the cell size to provide high bandwidth coverage implies a significant increase in power demand due to massive installation of RAUs. Although the efficiency of PoF is lower than that of using the traditional copper wires, it is able to dynamically adjust the supply power according to the requirements of each RAU, which can effectively reduce the overall power consumption of the 5G network [8].

Over the years, the procedure of PoF transmission to RAUs based on double-clad fiber (DCF) [9], multi-mode fiber (MMF) [10], and multicore fiber (MCF) [11,12] have been demonstrated. Recently, optically powered RoF transmitting systems using a single mode fiber (SMF) have been demonstrated [6,7,13], which is of particular interest because the SMF is widely deploying in optical networks. Different wavelengths were used for the power transmission. The shorter wavelength of 830 nm [6] provides higher photovoltaic conversion efficiency, which is inversely proportional to the wavelength, while the longer wavelength of 1064.8 nm [13] has lower losses in the optical fiber. The error-vector magnitude is usually used to describe an influence of high power light on optically carried information signals. This is a complex digital signal transmission characteristic that generally depends on the modulation format. Thus, more general criteria independent of the modulation format are needed to evaluate optically powered RoF transmission systems.

We proposed an original SMF-based PoF configuration and have investigating the achievable broadband analog transmission performance from an optically powered RAU with a high frequency external Mach-Zehnder modulator. The wavelength of 976 nm provides lower optical losses than 830 nm and can be converted by a cheaper and more reliable silicon photovoltaic converter, in contrast to the A3B5-based converter used in previous works. A commercially available 976 nm high power laser pump diode for erbium-doped fiber amplifiers was used. The primary analog signal transmission characteristics (gain, noise figure, and spurious-free dynamic range SFDR), independent of modulation formats, were used to determine the effect of strong light on the RF signal.

2. System Configuration

The scheme of the proposed RoF transmitting system with optically powered RAU is shown in Figure 1. The RAU is based on a dual output lithium niobate Mach-Zehnder modulator (LN MZM) [14]. The titanium in-diffused optical waveguides [15] form an optical scheme of the LN MZM. To accurately balance the modulator outputs, we used an original technique for precise photorefractive trimming of X-type waveguide directional coupler [16]. Push-pull traveling-wave electrodes provide broadband modulation with a frequency band up to 20 GHz [17]. The LN MZM was set to the quadrature operating point by a specially designed electronic system [18], which equalized the constant optical power at different outputs of the modulator by applying a control DC voltage to the bias electrodes.

The analog optical link included an optical carrier source and a balanced photodetector at the central station (CS) in addition to LN MZM as a RAU. So-called quasi-depolarized source [19] consisting of two laser diodes with distributed feedback was used as an optical carrier source. Low-noise single-frequency laser diodes with relative intensity noise (RIN) lower than -160 dB/Hz were used. Radiation from the diodes was combined into one standard SMF in the form of two orthogonal polarization components of equal amplitude using a fiber polarization combiner, which eliminates the polarization fading caused by LN MZM anisotropy. The wavelengths of laser diodes were chosen so that the frequencies of the interference beats were outside the band of transmitted high-frequency information signals.

The balanced detector was assembled from two chips of broadband photodiodes. Diodes with a saturation current of 30 mA were taken to operate with a sufficiently high optical power. The diodes were selected with the same response efficiency and similar spectral characteristics to provide high common-mode noise rejection (about 20 dB). Note that in the balanced detector scheme, the frequency response bandwidth was two times narrower compared to the bandwidth of responses of each photodiode separately, which was 10 GHz.

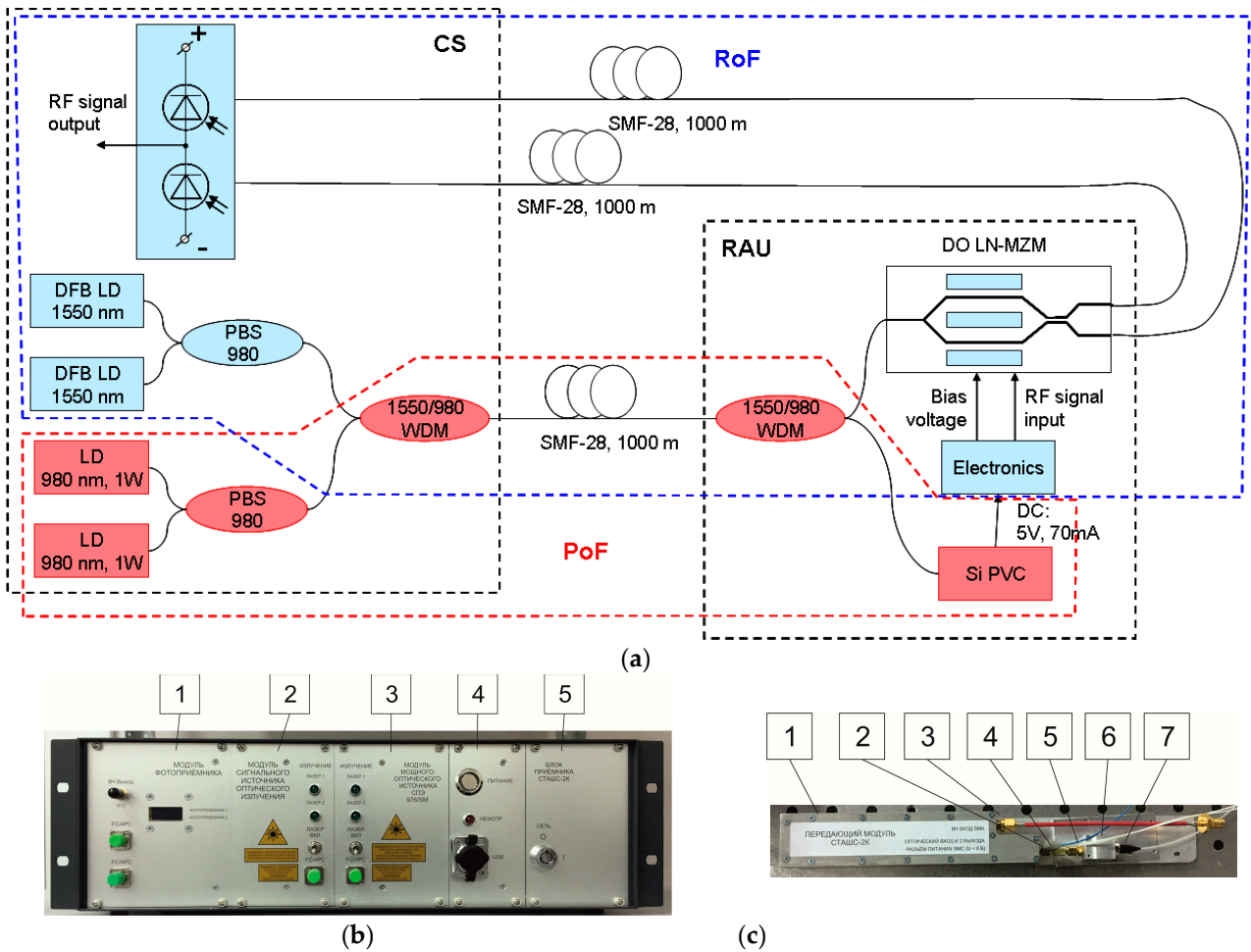


Figure 1. (a) Schematic diagram of the proposed system based on the RoF technology with optically powered RAU. (b) Central station (CS) layout: 1—balanced photodetector, 2—quasi-depolarized source optical carrier source (1550 nm), 3—high power light source (976 nm), 4—control electronics, 5—power supply. (c) Remote antenna unit (RAU): 1—LN MZM with operation point control electronics, 2—optical carrier input (blue fiber) and RoF signal output (white fiber), 3—RF signal input, 4—power input, 5—electrical output of the photovoltaic converter, 6—Si-based photovoltaic converter, 7—optical input of the photovoltaic converter.

The PoF system used two 1 W laser diodes at a wavelength of 976 nm. These are the standard pump lasers for erbium doped fiber amplifiers (EDFA), which have also been multiplexed with a polarization combiner. The wavelength was chosen as a tradeoff between optical-to-electrical conversion efficiency of the photovoltaic power converter, which is inversely proportional to the wavelength and optical loss in SMF, with the minimum at 1550 nm. The wavelength spacing between the high-power light and the signal optical carrier was large enough to avoid the high-power light transformation to the signal light due to nonlinear effects such as stimulated Raman scattering.

The high power light and signal optical carrier were combined in the 1 km single SMF fiber (Corning SMF-28e) with a core diameter of 8.2 μm using 1550/980 nm wavelength division multiplexer (WDM), which is commonly used in EDFA for pump launching. The same 1550/980 WDM was used to separate them at LN MZM input. Silicon multi-junction photovoltaic converter (YCH-H003, MH GoPower) was used for optical to electrical conversion. An acceptable temperature regime of the converter was provided by passive cooling using an aluminum radiator.

Thus, only standard commercially available telecom components have been used in the proposed cost-effective approach for the co-transmission of high-power light and signal optical carrier.

3. PoF System Efficiency

The power transfer efficiency is a product of optical-to-electrical conversion efficiency of the photovoltaic power converter and optical loss, which is attributed to the insertion loss of the used fiber optical components such as the 1550/980 WDM and the transmission loss of SMF at 976 nm. Figure 2 a presents the optical power at the input of photovoltaic power converter after transmission of the high power light over 1-km SMF versus optical power at the input 1550/980 WDM. A linear dependence with a slope corresponding to about 70% of the optical transmission efficiency indicates good suppression of nonlinear effects, especially stimulated Brillouin scattering. Figure 2b shows the I–V characteristic of the photovoltaic converter at the maximum (1.4 W) optical power at its input. An electrical power of 350 mW (5 V, 70 mA) can be obtained, which is sufficient for the power supply of the electronic system for control and stabilization of the modulator operation point and high-frequency low noise preamplifier.

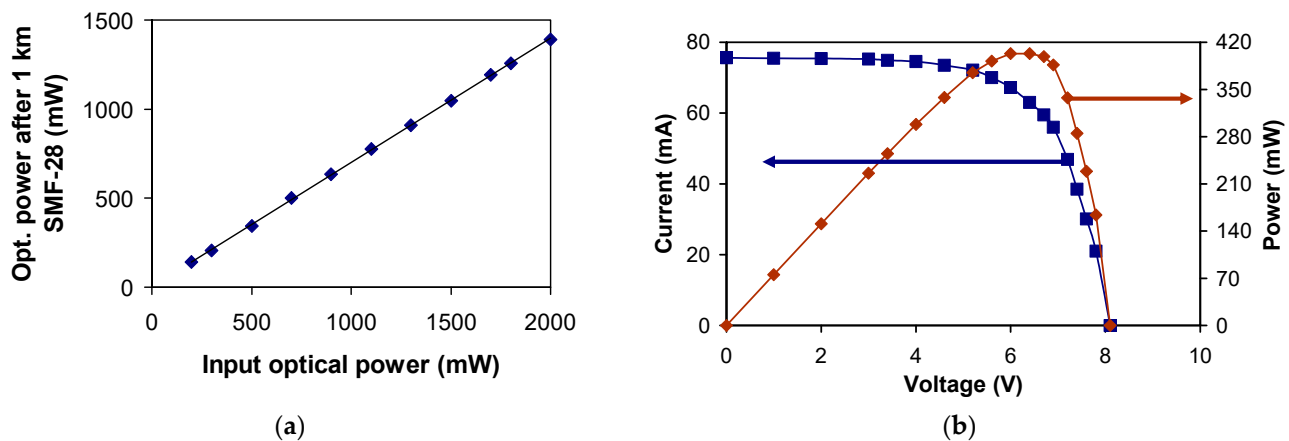


Figure 2. (a) 976 nm transmission efficiency through 1 km SMF-28 optical fiber. (b) I–V characteristic of the photovoltaic converter.

Some light at wavelength of 976 nm penetrates through the output 1550/980 WDM to the input of LN MZM and potentially could provide excessive noise in high-frequency signal carried at 1550 nm.

4. High Frequency Analog Signal Transmission Performance

The performance of analog optical links is usually evaluated using the same parameters that are used to characterize other radio frequency components [20]. The primary ones are: (1) gain; (2) bandwidth; (3) noise figure (NF); and (4) spur-free dynamic range (SFDR). Let us highlight the key features of the system under investigation. Dispersion and nonlinearity in the fiber have a negligible effect on link performance due to a short length of fiber optic link (1 km). The performance of only so-called intrinsic link was measured. The intrinsic link consists of a modulation device and a demodulation device with passive components for impedance matching and a short (1 km) fiber optic cable to connect them. We deliberately exclude any amplification, both RF and optical, to avoid their interfering effects (addition noise and nonlinear distortion), thereby increasing the visibility for an influence of the high-power light transmission on the link parameters.

The proposed fiber optic link was tested in two modes. In the first mode of amplitude modulation with direct detection (the standard mode), only one LN MZM output was connected to one photodiode of the balanced photodetector. There is no noise suppression in this mode, and the effect of high-power light transmission should be more noticeable. The

second mode used two arms and demonstrated effective noise suppression (the balanced mode). Note that for effective noise suppression, the optical lengths of the two arms must be equal.

Let’s start by measuring frequency dependence of the link gain (Figure 3). A rather high gain was associated with a high power of the signal laser diodes. The gain in balanced mode was 6 dB higher than in standard mode, as predicted by theory [21]. The increase in gain in the balanced mode is associated with a twofold increase in the total optical power of the carrier after LN MZM and the summation of the signal amplitudes in two arms. The frequency range was mainly determined by the bandwidth of the photodetector and was somewhat narrower for the balanced mode due to some difference in the lengths of the arms. No noticeable effect of powerful light on the gain was observed in both operating modes.

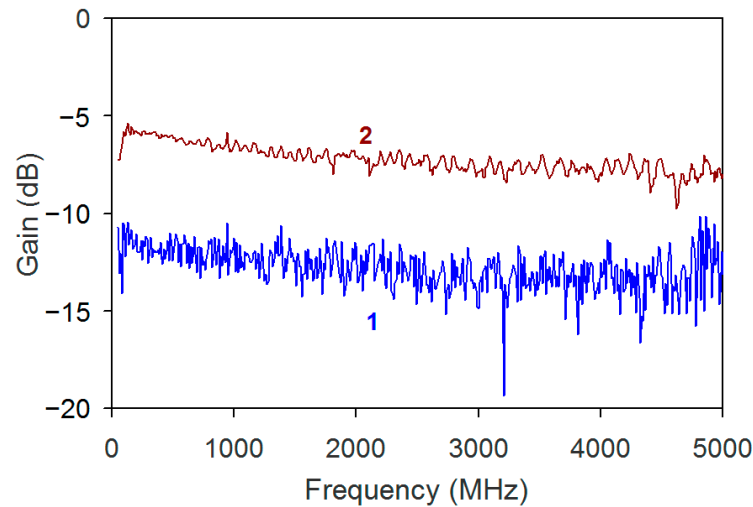


Figure 3. Frequency dependence of the optic link (gain). (1) is the standard mode of amplitude modulation with direct detection, (2) is the balanced mode.

The noise performance was characterized by the noise figure (NF), which is the degradation of signal-to-noise ratio (SNR) when input noise is the thermal noise generated at 290 K [19]. Firstly, the optical noise power density (Figure 4a) was measured at the input of LN MZM. A noticeable increase in the noise power density was observed when the high-power lasers at 976 nm were switched on. This addition noise is related to a penetration of light with a wavelength of 976 nm through 1550/980 WDM. NF was above 30 dB (Figure 4b) without noise suppression and reduced lower than 25 dB in the balanced mode. The so-called “shot noise limit”, when shot noise dominates the power spectral density of the output noise, can be estimated using the expression for the shot noise power spectral density [21]:

$$N_{sh} = 2qI_{DC}R|H|^2 \tag{1}$$

where $q = 1.6 \times 10^{-19}$ C is the electron or elementary charge, I_{DC} is the DC current on the photodetector, R is the load resistance (50 Ω), and H is the sensitivity of photodetector (typical value is $\frac{1}{2}$), which generally depends on RF frequency. Expression (1) in the decibel form rewritten as:

$$N_{sh}[dB/Hz] = -174 - 10\log(I_{DC}[mA]) \tag{2}$$

−174 dB/Hz is the thermal noise of the load resistance of 50 Ω. The noise factor can be calculated from the standard definition [21]:

$$N_{sh}[dB/Hz] = 22.1 - 10\log(I_{DC}[mA]) + 20\log(V_{\pi}[V]) \tag{3}$$

where V_{π} is a half wave voltage of the LN MZM. For the parameters of our RoF system ($I_{DC} = 13$ mA and $V_{\pi} = 3.5$ V), NF in the shot noise limit is estimated to be 22 dB. The experimentally achieved value was about 25 dB, which is only 3 dB higher. Thus, the additional noise caused by high optical power transmission in the PoF system could be suppressed efficiently by balancing detection and weakly affects the transmission of broadband analog radiofrequency signals.

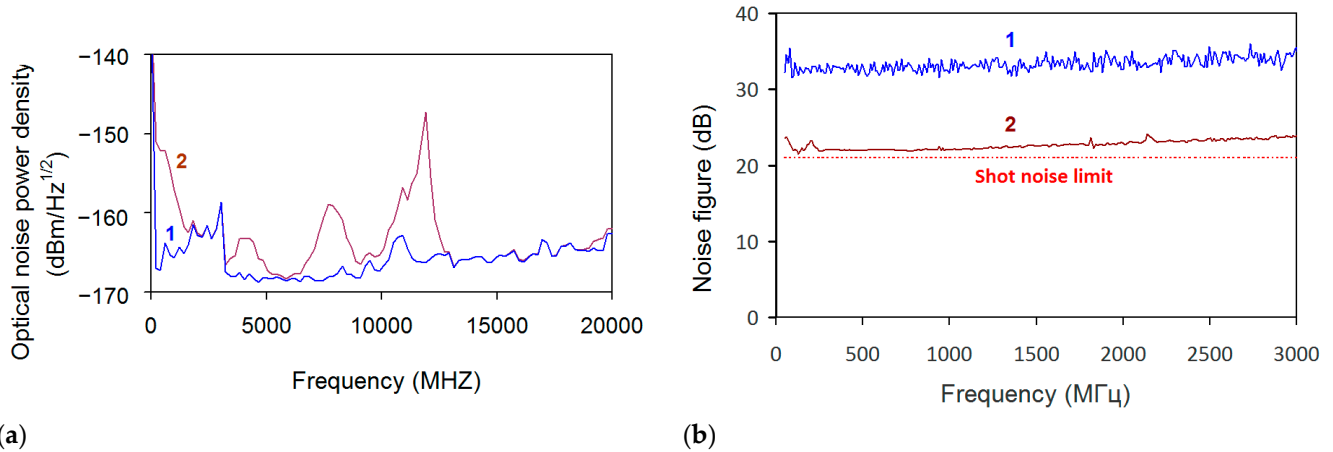


Figure 4. (a) The optical noise power density versus radio frequency: (1)—976 nm LD is switched off, (2)—976 nm LD is switched on. (b) Noise figure as a function of signal frequency (1) is the standard mode of amplitude modulation with direct detection; (2) is the balanced mode.

Figure 5 shows the spurious free dynamic range, which was about 110 dB/Hz^{2/3} for the standard link and increased to the 117 dB/Hz^{2/3} for the balanced configuration.

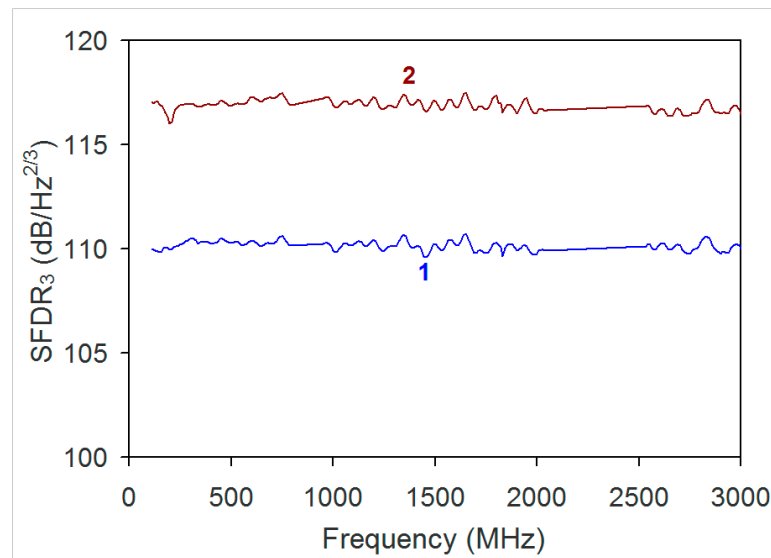


Figure 5. The spurious free dynamic range as a function of signal frequency; (1) is the standard mode of amplitude modulation with direct detection, and (2) is the balanced mode.

5. Conclusions

To summarize, light with a power of more than 2 W with a wavelength of 976 nm was used in the PoF system over a distance of 1 km with a standard single-mode fiber. Electrical power up to 350 mW (5 V, 70 mA) was obtained from a multi-junction silicon photocell, resulting in an optical transmission efficiency of about 70% and a photocell efficiency of 25%. These results are comparable to previous results of simultaneous transmission of 1064.8 nm high-power light and 1550 nm 5G NR 64QAMOFDM optical signal over 1 km

single-mode fiber [13]. Note that for a given power delivery distance, there is an optimum wavelength with maximum transmission efficiency, which is a compromise between optical fiber loss, with a minimum at 1550 nm, and photovoltaic converter efficiency, which is inversely proportional to wavelength. The additional advantage of the wavelength (976 nm) is the availability of standard commercially available fiber optic components, laser diodes for EDFA pumping, and a cheaper and more reliable silicon-based photovoltaic converter, making our approach very cost-effective. The maximum transmitted optical power may be increased in the future by wavelength multiplexing.

Power transmission of light with a wavelength of 976 nm was carried out simultaneously with transmission of the optical carrier at 1550 nm to a remote modulator. High-power light with a wavelength of 976 nm only slightly affects the transmission of the high-frequency analog signal. Additional noise caused by high optical power transmission in the PoF system can be suppressed efficiently by balancing the detection. Key broadband analog transmission characteristics such as noise figure ($NF < 25$ dB) and spurious-free dynamic range ($SFDR_3 > 117$ dB/Hz^{2/3}) close to the fundamental shot noise limit were achieved.

The approach reported in this work is promising for powering a remote antenna unit in optical fronthaul architecture. The use of transmitted power for signal amplification and improvement of RoF performance is the subject of future research and system optimization.

Author Contributions: Conceptualization, P.A., M.P. and A.S.; methodology, A.V., P.A. and M.P.; validation, A.S.; formal analysis, P.A. and A.S.; investigation, A.V., M.P., A.T., I.I. and A.U.; writing—original draft preparation, A.S.; writing—review and editing, P.A. and A.S. All authors have read and agreed to the published version of the manuscript.

Funding: This research received no external funding.

Institutional Review Board Statement: Not applicable.

Informed Consent Statement: Not applicable.

Data Availability Statement: The data are available from the first author and the corresponding author upon reasonable request.

Conflicts of Interest: The authors declare no conflict of interest.

References

1. DeLoach, B.C.; Miller, R.C.; Kaufman, S. Sound alerter powered over an optical fiber. *Bell Syst. Tech. J.* **1978**, *57*, 3309–3316. [[CrossRef](#)]
2. De Nazare, F.V.B.; Werneck, M.M. Hybrid optoelectronic sensor for current and temperature monitoring in overhead transmission lines. *IEEE Sens. J.* **2012**, *12*, 1193–1194. [[CrossRef](#)]
3. Bottger, G.; Dreschmann, M.; Klamouris, C.; Hubner, M.; Roger, M.; Bett, A.W.; Kueng, T.; Becker, J.; Freude, W.; Leuthold, J. An Optically Powered Video Camera Link. *IEEE Photon. Technol. Lett.* **2008**, *20*, 39–41. [[CrossRef](#)]
4. Budelmann, C. Opto-electronic sensor network powered over fiber for harsh industrial applications. *IEEE Trans. Ind. Electron.* **2018**, *65*, 1170–1177. [[CrossRef](#)]
5. Sakano, T.; Fadlullah, Z.M.; Kato, N.; Takahara, A.; Kumagai, T.; Kasahara, H.; Kurihara, S. Disaster-Resilient Networking: A New Vision Based on Movable and Deployable Resource Units. *IEEE Netw.* **2013**, *27*, 40–46. [[CrossRef](#)]
6. Wake, D.; Nkansah, A.; Gomes, N.J.; Lethien, C.; Sion, C.; Vilcot, J.P. Optically powered remote units for radio-over-fiber systems. *J. Lightwave Technol.* **2008**, *26*, 2484–2491. [[CrossRef](#)]
7. Al-Zubaidi, F.M.A.; López Cardona, J.D.; Montero, D.S.; Vázquez, C. Optically Powered Radio-Over-Fiber Systems in Support of 5G Cellular Networks and IoT. *J. Lightwave Technol.* **2021**, *39*, 4262–4269. [[CrossRef](#)]
8. Ashraf, I.; Boccardi, F.; Ho, L. SLEEP mode techniques for small cell deployments. *IEEE Commun. Mag.* **2011**, *49*, 72–79. [[CrossRef](#)]
9. Matsuura, M.; Tajima, N.; Nomoto, H.; Kamiyama, D. 150-W Power-Over-Fiber Using Double-Clad Fibers. *J. Lightwave Technol.* **2020**, *38*, 401–408. [[CrossRef](#)]
10. Kuboki, H.; Matsuura, M. Optically powered radio-over-fiber system based on center- and offset-launching techniques using a conventional multimode fiber. *Opt. Lett.* **2018**, *43*, 1057–1070. [[CrossRef](#)] [[PubMed](#)]
11. Vázquez, C.; López-Cardona, J.D.; Lallana, P.; Montero, D.S.; Al-Zubaidi, F.M.A.; Pérez-Prieto, S.; Garcilópez, I.P. Multicore fiber scenarios supporting power over fiber in radio over fiber systems. *IEEE Access* **2019**, *7*, 158409–158418. [[CrossRef](#)]
12. Yang, H.; Wang, S.; Qin, Y.; Fu, S. Optically powered 5G WDM fronthaul network with weakly-coupled multicore fiber. *Opt. Express* **2022**, *30*, 19795–19804. [[CrossRef](#)] [[PubMed](#)]

13. Yang, H.; Peng, D.; Qin, Y.; Li, J.; Xiang, M.; Xu, O.; Fu, S. 10-W power light co-transmission with optically carried 5G NR signal over standard single-mode fiber. *Opt. Lett.* **2021**, *46*, 5116–5119. [[CrossRef](#)] [[PubMed](#)]
14. Petrov, V.M.; Agruzov, P.M.; Lebedev, V.V.; Il'ichev, I.V.; Shamray, A.V. Broadband integrated optical modulators: Achievements and prospects. *Phys. Usp.* **2021**, *64*, 722–739. [[CrossRef](#)]
15. Parfenov, M.; Agruzov, P.; Il'ichev, I.; Shamray, A. Simulation of Ti-indiffused lithium niobate waveguides and analysis of their mode structure. *J. Phys. Conf. Ser.* **2016**, *741*, 012141. [[CrossRef](#)]
16. Parfenov, M.V.; Tronev, A.V.; Ilichev, I.V.; Agruzov, P.M.; Shamrai, A.V. Precise correction of integrated optical power splitters based on lithium niobate substrates by photorefractive effect local excitation. *Appl. Phys. B—Lasers Opt.* **2020**, *126*, 93. [[CrossRef](#)]
17. Lebedev, V.V.; Il'ichev, I.V.; Agruzov, P.M.; Shamray, A.V. The influence of the current-carrying electrode material on the characteristics of integral optical microwave modulators. *Tech. Phys. Lett.* **2014**, *40*, 743–746. [[CrossRef](#)]
18. Petrov, A.; Tronev, A.; Agruzov, P.; Shamrai, A.; Sorotsky, V. System for Stabilizing an Operating Point of a Remote Electro-Optical Modulator Powered by Optical Fiber. *Electronics* **2020**, *9*, 1861. [[CrossRef](#)]
19. Burns, W.K.; Moeller, R.P.; Bulmer, C.H.; Greenblatt, A.S. Depolarized source for fiber-optic applications. *Opt. Lett.* **1991**, *16*, 381–383. [[CrossRef](#)] [[PubMed](#)]
20. Cox, C.H.; Ackerman, E.I.; Betts, G.E.; Prince, J.L. Limits on the performance of RF-over-fiber links and their impact on device design. *IEEE Trans. Microw. Theory Tech.* **2006**, *54*, 906–920. [[CrossRef](#)]
21. Urlick, V.J.; Williams, K.J.; McKinney, J.D. *Fundamentals of Photonics*; John Wiley & Sons: Hoboken, NJ, USA, 2015; p. 496.

Disclaimer/Publisher's Note: The statements, opinions and data contained in all publications are solely those of the individual author(s) and contributor(s) and not of MDPI and/or the editor(s). MDPI and/or the editor(s) disclaim responsibility for any injury to people or property resulting from any ideas, methods, instructions or products referred to in the content.